ELSEVIER

Signal Processing: *Image Communication* 16 (2001) 531–540

SIGNAL PROCESSING: IMAGE COMMUNICATION

www.elsevier.nl/locate/image

Video image transmission over mobile satellite channels☆

Wendy X. Wang, Steven D. Blostein*

Department of Electrical and Computer Engineering, Queen's University, Kingston, Ontario, Canada K7L 3N6

Received 24 August 1998; received in revised form 18 September 1999

Abstract

This paper addresses the transmission of low bit-rate video image sequences through mobile satellite channels to provide portable communications services to remote areas. The particularly challenging aspects of this transmission channel include (1) rapid fading and log-normal shadowing, (2) low signal-to-noise ratio (SNR) due to the noise-limited channel, (3) the satellite's geostationary orbit which incurs a large 250 ms roundtrip propagation delay, (4) limited existing bandwidth near 2 GHz; the video service is to overlay existing Mobile Satellite (MSAT) voice service using a minimum number of 6 kHz (analog bandwidth) channels, and (5) the use of travelling-wave-tube amplifiers which preclude the bandwidth-efficient quadrature amplitude modulation (QAM) proposed for terrestrial high-definition TV (HDTV) broadcast. In the proposed concatenated system, the inner codec is compatible with both voice as well as future-oriented error-resilient, scalable video compression schemes. The key issues are the joint design of on-line channel estimation, soft-decision decoding, trellis-coded modulation (TCM), interleaving depths, and error correcting codes. We have shown through end-to-end bit-level simulation, that highly reliable transmission of 24 and 64 kbps video (H.263) can be realized at 15 and 40.5 kBd, respectively, with low delay, power and modest overall system complexity. © 2001 Elsevier Science B.V. All rights reserved.

Keywords: Satellite communications; Video image compression; Mobile communications; Wireless communications; Error control coding

1. Introduction

Although a number of systems have been proposed for the transmission of video over terrestrial mobile channels subject to multipath fading, none are particularly suited to mobile satellite transmission. One possible approach involves layered error protection [12,3] in which a coded video data stream is split, prioritized and separately protected using forward error correction or an automatic repeat request (ARQ) protocol. However, a mobile satellite channel that employs a geostationary satellite link has delay requirements that are too stringent to support an ARQ feedback-re-transmission iteration. It is also worth noting that the multi-stream data partitioning overhead may increase as the bit-rate is lowered. Although a multi-layer error protection approach has been shown to be promising for personal communications systems, at least for very low (1 Hz) pedestrian Doppler fading rates [12], the performance in the more rapid fading

☆This research has been supported by the Telecommunications Research Institute of Ontario.

* Corresponding author. Tel: +1-613-533-6561; fax: +1-613-533-6615.

E-mail address: sdb@ee.queensu.ca (S.D. Blostein).

0923-5965/01/$ - see front matter © 2001 Elsevier Science B.V. All rights reserved.
PII: S0923-5965(00)00034-5

encountered at vehicular speeds in general mobile satellite applications is an open question.

Both error control coding and ARQ can be avoided by expanding transmission bandwidth through subband source coding with built-in error resiliency [17]. However, this proves costly in narrowband applications, as will be quantified later. Although the approach in [17] results in a low power receiver implementation, the problem of low power transmission also needs to be addressed, a capability required for video conferencing of remote video links from moving platforms.

The mobile satellite channel has different modulation requirements than that of terrestrial systems which has impact on overall system design. Stedman et al. [20] and Streit and Hanzo [21] have proposed a mobile video transmission system based on highly bandwidth efficient quadrature amplitude modulation (QAM) for cellular application. QAM constellations have also been proposed for terrestrial HDTV broadcast. However, QAM transmission cannot be applied to the satellite channel since constant envelope modulation is required to allow travelling wave tube power amplifiers on the satellite transponder to operate in their linear region.

Other related research on robust transmission of video over mobile channels involve the development of subband coding algorithms optimized for low bit-rates [17–19,22]. Error resiliency can be achieved by a fixed length coding of quantized subband image blocks. Their main advantage is scalability. To increase the bandwidth efficiency of subband codecs, motion compensation-subband codecs have been proposed [18,22] with overall complexity approaching that of hybrid motion-compensated codecs. Their primary advantage over hybrid codecs, however, is scalability rather than bandwidth efficiency.

The objective of this paper is to evaluate the impact of integrating different source and channel coding strategies for video transmission over mobile satellite links. Previous studies have been carried out to determine the applicability of TCM to voice transmission over the mobile satellite channel, including [16,23], where bit error rates (BER) of 10^{-3}–10^{-4} have been achieved at an SNR, in terms of E_b/N_0, ranging from 9 to 11 dB. A much lower BER is required for video. A well-studied method to improve transmission reliability is by employing concatenated coding. In [26], a Reed–Solomon (RS) code, concatenated with TCM, is proposed for Rician and Rayleigh multipath fading channels. However, the analytical and experimental results in [26] are limited to the case of perfect fading phase information. In this paper, we address channel estimation to enable the use of coherent phase modulation in the fading channel. More significantly, rather than treating video information as generic data with a target BER, we have undertaken a subjective evaluation of image quality through a complete end-to-end bit-level simulation. Besides increased rate-distortion information, a further advantage of end-to-end simulation over many analytical performance studies is that finite interleaving performance can be directly evaluated so that the actual transmission delay can be traded-off against performance.

In the following, the channel model is first described in Section 2, two concatenated coding systems are proposed in Section 3, including an assessment of different channel state estimators. Section 4 reports the results of a complete end-to-end software emulation of the full concatenated coding system, including comparisons with an error resilient combined source and channel coding scheme of [17] as well as its 3D extension. In Section 5, the final discussion comments on low power implementation issues.

2. Channel model

Mobile satellite channels are distorted by multipath fading, Doppler frequency shift and attenuation of line-of-sight (LOS) from foliage [15]. Rician or shadowed Rician [15] fading can be used to mathematically model the distortion on the channel, which is often referred to simply as fading. The distortion is particularly severe in northern latitudes such as in Canada where the angle between the LOS and the horizon is 15–20°. Typically, a Rician model assumes a constant LOS, whereas in a shadowed Rician process the LOS is lognormally distributed. It has been shown that a third-order Butterworth low pass filter [23] gives a close match with experimental second-order statistical satellite

Table 1
Shadowed Rician model parameters

Parameter	Light	Average	Heavy
b_0	0.158	0.126	0.0631
μ_0	0.115	−0.115	−3.91
$\sqrt{d_0}$	0.115	0.161	0.806

channel measurements [15]. At time k, the received symbol y_k is related to the transmitted symbol x_k by

$$y_k = c_k x_k + n_k, \tag{1}$$

where c_k is the complex fading channel gain and n_k is complex additive white Gaussian noise. The c_k are generated by three independent random variable sequences. The 3 dB cutoff frequency of the third-order Butterworth filters is equal to the normalized Doppler frequency f_0 and the filter frequency response is

$$|H(f)|^2 = \frac{3}{2\pi f_0} \frac{1}{1 + (f/f_0)^6}. \tag{2}$$

This filter spectrum has unit energy gain; that is, the total area under $|H(f)|^2$ is unity. Given the above fading frequency spectrum, the output normalized autocorrelation is given by [27]

$$\rho(\tau) = \tfrac{1}{2}[\exp(-2\vartheta) + \exp(-\vartheta)(\sqrt{3}\sin(\sqrt{3}\vartheta) + \cos(\sqrt{3}\vartheta))], \tag{3}$$

where $\vartheta = |\pi f_0 \tau|$. The complex channel gain c_k, for the shadowed Rician model is given by [15]

$$\overline{|c_k|^2} = \exp(2\mu_0 + 2d_0) + 2b_0. \tag{4}$$

The model parameters μ_0, d_0 and b_0 have been determined experimentally and are given in Table 1 for light, average as well as heavy shadowing. Our investigation concentrates on light and average shadowing indicative of a light to medium forested area.

3. Concatenated coding system

The source–channel coding theorem [8, Theorem 8.13.1] which applies stationary sources and discrete memoryless channels, states that source code and channel codes can be designed separately and then concatenated to achieve optimal performance. However, the sources and channels considered here are not stationary or memoryless. In fact, performing source and channel coding jointly may decrease system complexity, as demonstrated in [17]. Wei [29] proposed an unequal error protection scheme for additive white Gaussian noise channels (AWGC) with a nonuniformly spaced signal constellation. In [29], the data from video source encoders are classified into different priority classes and each class is coded differently. This scheme, however, is not applicable for fading channels because transmission of video over a wireless link differs from a physical link in that there is no guaranteed reliable transmission rate in which higher priority information would experience a much lower BER than lower priority data; rather, mobile links are subject to deep fades where all data is equally subject to loss. Secondly, when the source is highly compressed, any extra overhead arising from prioritizing data streams becomes more significant. Finally, a joint source–channel coding system may be inflexible with respect to different sources, channels, source coding techniques, and channel coding techniques, which is required to support the transmission of multimedia.

Trellis-coded modulation (TCM) conserves bandwidth while achieving high coding gain. For example, it can be shown that a coding gain of 3.6 dB is achievable using 8-state, 8-PSK TCM over uncoded quadrature phase-shift keying (QPSK) [5,27]. The decoding of TCM is typically based on the Viterbi soft-decision decoding algorithm [5]. Trellis decoding branch metrics are computed over all possible data symbols x_k, e.g., we minimize

$$m(y_k, x_k) = |y_k - \hat{c}_k x_k|^2, \tag{5}$$

where $\hat{c}_k$ is the estimated fading channel gain and the other quantities are defined in Eq. (1). We remark that TCM has not been shown analytically to be optimum in channels with memory [11], as is the case where channels experience fading and finite interleaving is employed.

3.1. Channel estimation

Motivated by the need for bandwidth efficiency and coding gain within the constraints of the satellite channel, we propose 8-PSK modulation. Here, a phase reference is required to correctly demodulate the signal, i.e., we must estimate the complex gain c_k in Eq. (1), for all k. In the following, it is assumed that correct symbol timing information is received. It has been previously shown that for DSP-based satellite modems, the system degradation due to imperfect timing is less than 1 dB [4]. Rather, we incorporate the effects of imperfect channel estimation on system performance as well as compare five different techniques.

Pilot symbol-assisted techniques are both simple and well suited for channel estimation and involve periodically transmitting known symbols x_k to obtain estimates of c_k if n_k is small [6]. The simplest pilot-symbol-assisted (SA) technique, involves linear interpolation of the c_k between training symbols. To improve SNR (E_b/N_0) performance at the cost of increased delay, symbol-aided decision-directed (SADD) channel estimation can be used by incorporating decision feedback at the data samples [11]. As an alternative to linear interpolation, decision feedback with adaptive linear prediction (DFALP) has been shown analytically to improve BER performance for the case of fast Doppler fading channels [13]. A minimum delay channel estimator, the optimum one-step linear Kalman predictor, also has been proposed [9,27]. This scheme can be further enhanced with *soft* decision feedback using the *multiple model* algorithm [2,27]. All five techniques have been implemented and tested on the mobile satellite channel described in the previous section. Although space limitations prohibit detailed comparison among these five different techniques, Fig. 1 shows a representative plot of the BER performance of the different techniques as applied to the mobile satellite channel for the case of uncoded QPSK modulation. A detailed comparative study can be found in [27]. From Fig. 1, it can be seen that the simplest technique, SA, is the preferred compromise for the mobile satellite channel. We note that the added delay of all channel estimation schemes are all small (no more than 20 ms) as compared to that of the channel roundtrip delay. As a result, the added complexity and SNR performance cost of DFALP as well as the Kalman-based predictors to reduce the delay further cannot be justified. In addition, Fig. 1 generally agrees with the conclusions in [11,13] that decision feedback cannot improve BER performance appreciably at these low SNR values.

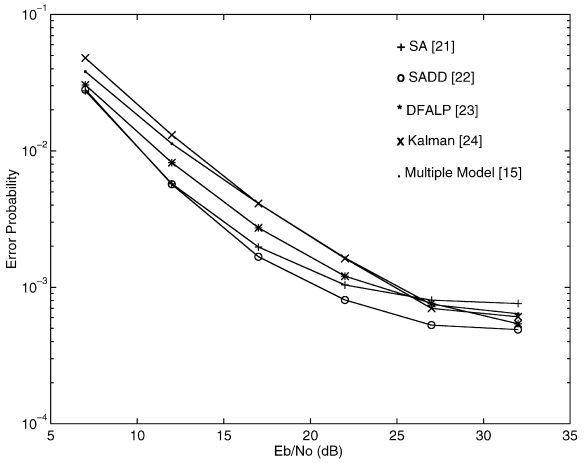

Fig. 1. BER for SA, SADD, DFALP, Kalman filtering, multiple model algorithm in light shadowed Rician fading, normalized fading bandwidth at 0.05, pilot symbol rate at 5, uncoded QPSK modulation.

In the SA channel estimator employed in later sections, one training symbol is sent for every 9 data symbols ($k_t = 10$), a value that is able to track the fading gain of high-speed vehicles while adding only modest transmission overhead. The normalized Doppler frequency, f_0, corresponding to a carrier frequency of 2.5 GHz and a vehicle speed of 100 km/h for 24 and 64 kbps data rates are 0.015432 and 0.005787, respectively.

3.2. Error-control coding

It is well known that in fading channels employing soft-decision decoding of convolutional codes such as in TCM, errors tend to occur in bursts. Multiple error correction capability of forward error correcting (FEC) codes such as that of the RS or Bose–Chaudhuri–Hocquenghem (BCH) codes [14] are therefore required. Fig. 2 shows the concatenated coding block diagram, consisting of video

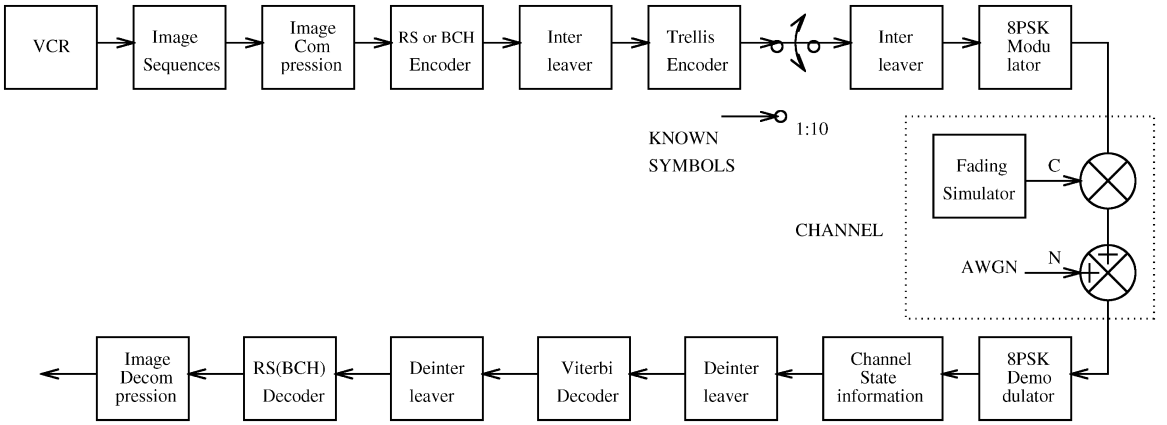

Fig. 2. Concatenated coding system block diagram. Source coding (compression) is followed by outer (RS or BCH) error control coding, outer interleaving, trellis coding, pilot symbol insertion, inner interleaving.

image compression followed by outer FEC, optional outer interleaving, inner TCM, pilot symbol insertion, inner interleaving and 8-ary phase shift keying (8-PSK) modulation. The inner interleaving is performed to spread the TCM-induced error bursts. Also, in satellite communication systems, the long roundtrip delay severely limits the possible depth of outer interleaving.

We propose a concatenated coded modulation scheme where the inner code is a 2/3 rate, 8-state 8-PSK TCM [24], SA channel estimation, an inner interleaver with depth dependent on symbol rate, no outer interleaving and an outer FEC consisting of a (255, 223) standard NASA RS code. We refer to this as System 1. In System 1 no outer interleaver is used due to the large delay incurred by the RS code. We note that the RS block code (255×8 bits) can correct 16 8-bit symbol errors, i.e., 128-bit burst errors.

We have compared System 1 to an alternative concatenated system design that employs a simpler (255, 233) BCH outer code that can correct four bit errors. As expected, at comparable delays, the greater error correction capability of RS codes was observed. Therefore, an outer interleaver was added to the BCH system. When the outer interleaving depth exceeded 20 symbols, corresponding to a delay of 196 ms at 64 kbps, the BER performance of the BCH system started to exceed that of System 1, which has an overall delay of 89 ms at 64 kbps. For example, at 10 dB SNR, BERs of 2.90×10^{-5} and 5.81×10^{-5} were observed in light and average shadowing conditions, respectively, as compared to 3.84×10^{-5} and 7.41×10^{-5} for System 1. Similar results were observed at 12 dB SNR.

Motivated by the above, System 2 was chosen for detailed investigation that differs from System 1 in that the RS code is replaced with an outer (255, 223) BCH code combined with an outer interleaving depth of 80, which provides for improved SNR performance with a much greater delay penalty. Although not presented here, we note that the use of shorter outer codes are possible such as the BCH (31,16), which enables simpler implementation and low delay but at a cost of significant bandwidth expansion.

3.3. Inner coding performance

To quantify the effect of concatenated coding on the mobile satellite channel, Fig. 3 indicates that BERs of 10^{-3}–10^{-4} can be achieved by inner codes alone at SNR in the range of 9–11 dB. Inner interleaving depths of 30 and 60 symbols were used, for 24 and 64 kbps transmission, respectively.

By way of comparison, we have evaluated the inner-coded system performance in more conventional Rician and Rayleigh fading channels found in terrestrial systems. Although the Doppler

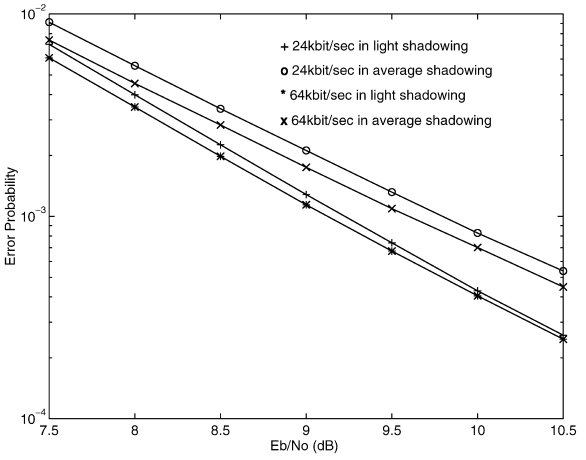

Fig. 3. Inner TCM code performance for 24 and 64 kbps, inner interleaving depths are normalized fading bandwidth at 0.0154 and 0.0057, respectively, SA channel estimation with pilot symbols every $k_t = 10$.

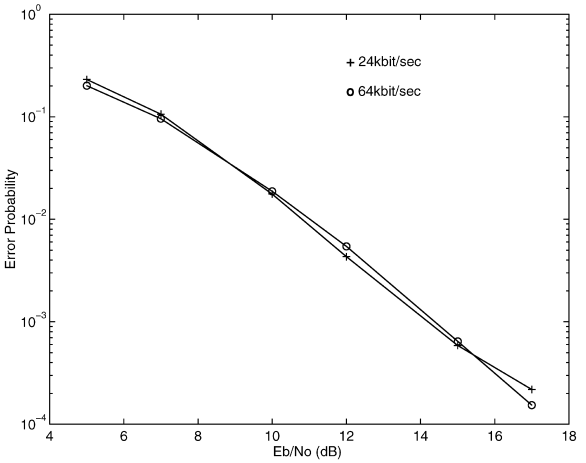

Fig. 4. Inner TCM code performance for 24 and 64 kbps over a Rayleigh channel with $k_t = 10$.

frequencies are the same under shadowed Rician, Rician and Rayleigh fading channels, the low-pass filter bandwidth used in the SA channel estimation algorithm must be set differently for the three different channels to assure maximum performance. Based on exhaustive search, it was found that the low-pass filter bandwidth should be set largest (no filtering) for Rayleigh fading, smallest (0.22) for the Rician ($K = 10$ dB) channel and 0.36 for shadowed Rician fading channel, where a bandwidth of 0.5 corresponds to a frequency of π rad/s. Comparing the results in Figs. 3 and 4 we note that a Rayleigh channel requires an additional channel SNR of approximately 5 dB to achieve the same inner TCM code performance. In addition, an extra SNR margin of 2 dB is required for a conventional Rician channel with a K-factor of 10 dB. See [27, Fig. 3.25].

3.4. Concatenated coding performance

In Fig. 3, the different normalized fading bandwidths result from different data rates of 24 and 64 kbps. The results in Figs. 5 and 6 show that for System 2 BER performance is around 1.5 dB better than that of System 1. We note that the BER results for System 2 at 24 and 64 kbps cannot be directly compared due to the use of different inner interleaving depths in each case. We also note that since the Doppler fading is faster for 24 rather than 64 kbps transmission, the error bursts are shorter resulting in more effective error correction by the RS code since no outer interleaving is employed in System 1. We note that the delay penalty for interleaving is too high for interactive video; the delay for the combined BCH-outer-interleaving-TCM system

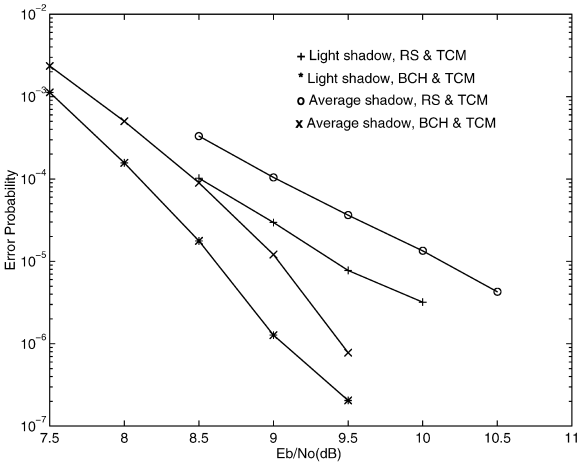

Fig. 5. Concatenated system performance at 24 kbps, normalized fading bandwidth at 0.0154, RS and TCM refers to System 1 while BCH and TCM refers to System 2. System 2 has depth 80 outer interleaver.

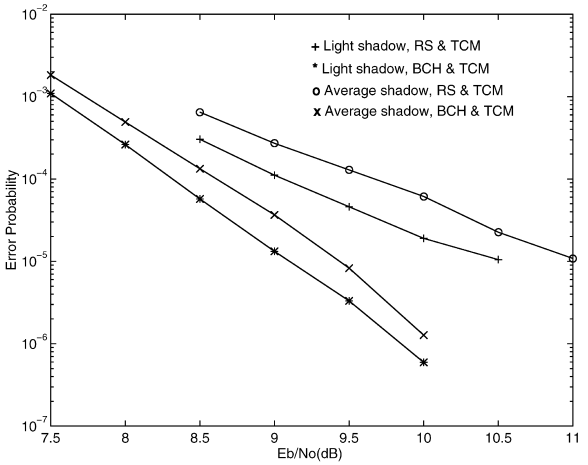

Fig. 6. Concatenated system performance at 64 kbps, normalized fading bandwidth at 0.0057, RS and TCM refers to System 1 while BCH and TCM refers to System 2. System 2 has depth 80 outer interleaver.

was 1.54 s and 615 ms, for 24 and 64 kbps, respectively, while for the RS-TCM system, the corresponding delays were only 145 and 89 ms, respectively. From Figs. 3, 5 and 6, further improvement of more than two orders of magnitude in BER performance at 9 dB SNR can be obtained over the inner coding system by employing either of the outer FEC codes.

For System 1 employing 24 and 64 kbps compressed image bit streams, respectively, the outer (255, 223) RS code yields a total bit-rate of 27.44 and 73.18 kbps, respectively, which correspond to symbol rates of 13.72 and 36.59 kBd respectively. After adding the pilot symbols ($k_t = 10$) the system baud rates become 15.2 and 40.5 kBd, respectively. The respective analog signal bandwidths are 15.2 and 40.5 kHz not including approximately 30% excess bandwidth required for pulse shaping to reduce intersymbol interference.

4. Overall system performance

We now describe the subjective image quality evaluation of System 1 proposed in the previous section. Monte-Carlo simulations of colour video image sequences at QCIF resolution (176×144 pels) in 4:1:1 YUV format were performed (Fig. 7, top left). Sequences of 150 frames, each at 30 frames/s, subsampled to 50 frames each at 10 frames/s, were transmitted repeatedly for 25 min (15 000 frames) of motion video at 24 kbps and 8 min of video at 64 kbps, respectively. The test video sequences included the well-known Miss America, Susie, Salesman, Mother and Daughter, Grandma, Carphone, Foreman, Claire, Stennis, and other sequences digitized locally.

The subjective video quality results revealed virtually error free performance at SNRs above 10 dB in light and average shadowing mobile satellite channels. Here, the BER was below 10^{-6} and channel errors were rare and had negligible effect on image quality. Thus, a 10 dB link margin seems to be a minimum for video satellite transmission, with inner FEC voice transmission compatibility. Fig. 7 shows one of the worst 200 error frames decoded out of a total of 15 000 video frames transmitted through an averaged shadowed mobile channel at a channel signal-to-noise ratio of 10 dB and BER of 1.4×10^{-5}. Above 11 dB, these visible errors had disappeared completely. From examining the video sequences, there are different error patterns present for different video sequences. For the low error rates encountered here (BER less than 6×10^{-5}), the H.263 source codec's periodic intra-frame updating strategy is robust enough to recover from errors. Because of the low channel BER, only a few frames, representing 20 s total duration in a 25 min sequence, exhibit visible burst errors (Fig. 7, bottom) and the remaining frames are error free and are reconstructed as in Fig. 7, top right. When the channel SNR is greater than 11 dB, the BER is less than 10^{-7} and there were no channel errors in the 25 min video sequences. The distortion displayed at the 10 dB point for average shadowing therefore represents a threshold SNR where the distorted bit stream can still be recovered by the codec. It is also interesting to observe the types of visible distortion that occur at 10 dB. This may be useful for designing error concealment techniques in the future.

We now compare the concatenated system (System 1 above) to one that employs error-resilient subband video image compression, as proposed in [17], which we refer to as System 3. We have also modified the subband codec in [17] by extending

Fig. 7. Top-left: Original luminance frame 108 of Susie at 9.1 mbits/sec. Top-right: Susie at compressed 24 kbps in average shadowed fading channel at 12 dB SNR, 15 kBd, 145 ms delay channel. This top right image is visually indistinguishable from the case of an error-free channel. Bottom-left: worst-case channel distortion in 15 000 frames at 10 dB SNR, 15 kBd, 145 ms delay channel.

the 2D subband decomposition to a 3D decomposition to obtain some performance improvement, as described in [28], which we refer to as System 4. The advantage of the subband codec relative to the concatenated Systems 1 and 2 is reduced implementation complexity; for the subband codec FEC is not required, while the inner TCM system remains the same. A comparison among Systems 1, 3 and 4 for the case of zero channel noise, in terms of PSNR and bit-rate, is shown in Table 2, where the 9-tap symmetric filter proposed in [1], is used for subbanding. First, it can be seen that where the 2D and 3D subband systems have the same PSNR, the 2D system's bit-rate is 28% greater. Second, we note that concatenated coding (System 1) achieves the same image quality at almost in order of magnitude savings in bit-rate; 112 kbps were required to transmit the same quality video without FEC by System 4 as 24 kbps using concatenated coding via System 1. Note that although there is a modest saving of FEC overhead in the case of the subband system, this does not offset the joint source/channel coding inefficiency. For the case of the average shadowed fading satellite channel described earlier, the threshold SNR for acceptable performance was 2 dB higher than that of the concatenated system.

5. Discussion

Our investigations using a software H.263 24 and 64 kbps codec, concatenated FEC coding and online channel state estimation show that robust moving-image transmission through shadowed

Table 2
Average PSNR performance comparison of error-resilient subband joint source/channel coding (Systems 3 and 4) and concatenated H.263 coding (System 1)[a]

Video	Joint source/channel			Concatenated H.263		
	2D Subband 0.6 bpp	3D Subband 0.6 bpp	0.47 bpp	(System 1) 0.063 bpp	0.095 bpp	0.25 bpp
Miss(QCIF)	31.73	33.88	32.23	36.66	37.95	39.82
Susie(QCIF)	30.29	32.14	30.49	31.46	33.16	36.28
Miss(CIF)	33.27	35.19	33.86			
Susie(CIF)	32.15	33.24	32.44			
Mark	31.38	32.23	31.31			

[a]2D and 3D subband coding achieve similar PSNRs at 0.6 and 0.47 bpp, respectively, while concatenated coding (System 1) has an order of magnitude lower bit-rate at similar PSNRs.

mobile satellite channels is feasible at low power, bandwidth and delay. Concatenated codes and pilot symbols result in a 15.2 kBd and 40.5 kBd rates, respectively, allowing for a near error-free image transmission at channel SNR above 10 dB. Depending on different system delay requirements, RS or BCH coding combined with 8-state 8-PSK TCM with symbol-aided channel estimation can be used for interactive transmission or one-way broadcasting applications, respectively.

A critical factor in the overall system design is power consumption, which determines the portability of the resulting video transceiver. Assuming that the majority of the power is consumed by (1) discrete cosine transform (DCT), (2) half-pel motion estimation (ME), (3) RS decoding and (4) TCM, and assuming the CMOS power dissipation model [7]:

$$P \approx CV^2 f, \tag{6}$$

where C denotes the effective loading capacitance, V the supply voltage (above least 2.9 V [31]) and f the operating clock frequency, and scaling the clock frequency according to (6) for operation at data rates corresponding to 24 and 64 kbps, respectively, we obtain the power consumption estimates shown in Table 3, assuming the entire system was integrated onto monolithic CMOS VLSI technology in the 1–1.8 μm range [10,25,30,31]. We note that low power consumption is mainly due to the low data rate, which lowers the operating system clock frequency. Thus, low bit-rate video can achieve low power despite the apparently high algorithm complexity. This conclusion is interesting in light of [17] where it was assumed from the outset that low power design should be achieved through a simple customized *error resilient* joint source and channel coding scheme. In the performance evaluation section, we showed that subband coding based on [17] requires approximately an order of magnitude greater data rate for the same amount of distortion.

Table 3
CMOS power requirements in mW

Algorithm	DCT	ME	RSD	TCM	Total power
24 kbps	0.70	1.54	0.17	2.26	4.67
64 kbps	1.86	4.11	0.46	6.04	12.47

References

[1] E.H. Adelson, E. Simoncelli, R. Hingorani, Orthogonal Pyramid Transforms for Image Coding, in: Proceedings of the SPIE, Cambridge, MA, October 1987, pp. 50–58.
[2] Y. Bar-Shalom, T.E. Fortmann, Tracking and Data Association, Academic Press, New York, 1988.
[3] B. Belzer, J. Liao, J.D. Villasenor, Adaptive video coding for mobile wireless networks, in: Proceedings of the IEEE ICIP, Vol. 2, Austin, TX, October 1994, pp. 972–976.
[4] M. Belanger, P.J. McLane, Measured flat fading performance of Doppler corrected Nyquist 4800 bps DQPSK modem, in: Proceedings of the IEEE International Conference on Communications, Seattle, USA, June 1995, pp. 1886–1890.

[5] E. Biglieri, D. Divsalar, P.J. McLane, M.K. Simon, Introduction to Trellis-Coded Modulation with Applications, Macmillan, New York, 1991.
[6] J.K. Cavers, An analysis of pilot symbol assisted modulation for Rayleigh fading channels, IEEE Trans. Veh. Technol. 40 (4) (November 1991) 687–693.
[7] A.P. Chandrakasan, S. Sheng, R.W. Brodersen, Low power CMOS digital design, IEEE J. Solid State Circuits 27 (4) (April 1992) 473–484.
[8] T.M. Cover, J.A. Thomas, Elements of Information Theory, Wiley, New York, 1991.
[9] Q. Dai, E. Shwedyk, Detection of bandlimited signals over frequency selective Rayleigh fading channels, IEEE Trans. Commun. 42 (3) (March 1994) 941–950.
[10] H. Dehash, R. Kerr, A.J. Viterbi, Practical applications of TCM, in: Proceedings of the IEEE MILCOM, Monterey, CA, 1990, pp. 380–383.
[11] G.T. Irvine, P.J. McLane, Symbol-aided plus decision-directed reception for PSK/TCM modulation on shadowed mobile satellite fading channels, IEEE J. Selected Areas Commun. 10 (8) (August 1992) 1289–1299.
[12] M. Khansari, A. Zakauddin, W.Y. Chan, E. Dubois, P. Mermelstein, Approaches to layered coding for dual-rate wireless video transmission, in: Proceedings of the IEEE ICIP, Vol. 1, Austin, TX, October 1994, pp. 258–262.
[13] Y. Liu, S.D. Blostein, Identification of frequency non-s elective fading channels using decision feedback and adaptive linear prediction, IEEE Trans. Commun. 43 (2–4) (April 1995) 1484–1492.
[14] S. Lin, D.J. Costello, Error Control Coding, Prentice-Hall, Englewood Cliffs, NJ, 1983.
[15] C. Loo et al., Measurements and modelling of land-mobile satellite signal statistics, in: Proceedings of the IEEE Vehicular Technology Conference, Dallas, USA, May 1986, pp. 262–267.
[16] P.J. McLane, P.H. Wittke, P.K.M. Ho, C. Loo, PSK and DPSK trellis codes for fast fading, shadowed mobile satellite communication channels, IEEE Trans. Commun. 36 (11) (November 1988) 1242–1246.
[17] T. Meng et al., Portable video-on-demand in wireless communication, Proc. IEEE 83 (4) (April 1995) 659–680.
[18] J. Ohm, Three-dimensional subband coding with motion compensation, IEEE Trans. Image Process. 3 (5) (September 1994) 559–571.
[19] C. Podilchuk, Low bit-rate subband coding, in: Proceedings of the IEEE ICIP, Vol. 3, Austin, TX, October 1994, pp. 280–284.
[20] R. Stedman, H. Gharavi, L. Hanzo, R. Steele, Transmission of subband-coded images via mobile channels, IEEE Trans. Circuits Systems Video Technol. 3 (1) (February 1993) 15–26.
[21] J. Streit, L. Hanzo, An adaptive discrete cosine transformed videophone communicator for mobile applications, in: Proceedings of the IEEE ICASSP, Detroit, MI, May 1995, pp. 2735–2738.
[22] D. Taubman, A. Zakhor, Multirate 3-D subband coding of video, IEEE Trans. Image Process. 3 (5) (September 1994) 572–588.
[23] C. Tellambura, Q. Wang, V.K. Bhargava, Performance of trellis coded modulation schemes on shadowed mobile satellite communication channels, IEEE Trans. Veh. Technol. 43 (2) (February 1994) 129–139.
[24] G. Ungerboeck, Trellis-coded Modulation with Redundant Signal Sets. Part I: Introduction; Part II: State of the Art, IEEE Commun. Mag. 25 (2) (February 1987) 5–21.
[25] S. Uramoto, T. Akihiko, A. Mitsuyoshi, S. Hiroki, Y. Mashiko, Half-pel precision motion estimation processor for NTCS-resolution video, Proceedings of the IEEE Custom Integrated Circuits Conference, San Diego, CA, 1993, pp. 11.2.1–4.
[26] B. Vucetic, Bandwidth efficient concatenated coding schemes for fading channels, IEEE Trans. Commun. 41 (1) (January 1993) 51–61.
[27] X. Wang, Video image tramsmission via mobile satellite channels, M.Sc. Thesis, Department of Electronics and Computer Engineering, Queen's University, Kingston, Ontario, Canada, 1995.
[28] X. Wang, S.D. Blostein, Three dimensional subband video transmission through mobile satellite channels, in: Proceedings of the ICIP, Vol. 3, Washington, DC, October 1995, pp. 384–387.
[29] L.F. Wei, Coded modulation with unequal error protection, IEEE Trans. Commun. 41 (10) (October 1993) 1439–1449.
[30] S.R. Whitaker, J.A. Canaris, K.B. Cameron, Reed Solomon VLSI codec for advanced television, IEEE Trans. Circuits Systems Video Technol. 1 (2) (June 1991) 230–236.
[31] A.Y. Wu, K.J. Liu, Low power and low-complexity DCT/IDCT VLSI architecture based on backward Chebyshev recursion, in: Proceedings of the IEEE Internat. Conf. on Circuits and Systems, Vol. 4, IEEE, London, 1994, pp. 155–158.